

Enhancing Generalization and Scalability for Multi-Objective Optimization with Population Pre-Training

Haokai Hong

haokai.hong@connect.polyu.hk

The Department of Data Science and Artificial Intelligence, The Hong Kong Polytechnic University, Hong Kong SAR, P.R. China

Liang Feng

liangf@cqu.edu.cn

The College of Computer Science, Chongqing University, Chongqing 400044, China.

Min Jiang

minjiang@xmu.edu.cn

The Department of Artificial Intelligence, Key Laboratory of Digital Protection and Intelligent Processing of Intangible Cultural Heritage of Fujian and Taiwan, Ministry of Culture and Tourism, School of Informatics, Xiamen University, Fujian, China, 361005.

Kay Chen Tan

kctan@polyu.edu.hk

The Department of Data Science and Artificial Intelligence, The Hong Kong Polytechnic University, Hong Kong SAR, P.R. China

Abstract

Multi-objective optimization problems (MOPs) require the simultaneous optimization of conflicting objectives. Real-world MOPs often exhibit complex characteristics, including high-dimensional decision spaces, many objectives, or computationally expensive evaluations. While population-based evolutionary computation has shown promise in addressing diverse MOPs through problem-specific adaptations, existing approaches frequently lack generalizability across distinct problem classes. Inspired by pre-training paradigms in machine learning, we propose a Population Pre-trained Model (PPM) that leverages historical optimization knowledge to solve complex MOPs within a unified framework efficiently. PPM models evolutionary patterns via population modeling, addressing two key challenges: (1) handling diverse decision spaces across problems and (2) capturing the interdependency between objective and decision spaces during evolution. To this end, we develop a population transformer architecture that embeds decision spaces of varying scales into a common latent space, enabling knowledge transfer across diverse problems. Furthermore, our architecture integrates objective-space features through objective fusion to enhance population prediction accuracy for complex MOPs. Our approach achieves robust generalization to downstream optimization tasks with up to 5,000 dimensions—five times the training scale and 200 times greater than prior work. Extensive evaluations on standardized benchmarks and out-of-training real-world applications demonstrate the consistent superiority of our method over state-of-the-art algorithms tailored to specific problem classes, improving the performance and generalization of evolutionary computation in solving MOPs.

Keywords

Evolutionary computation, multi-objective optimization, pre-trained model.

1 Introduction

Many optimization problems involve multiple conflicting objectives requiring simultaneous optimization (Deb et al., 2002). These multi-objective optimization problems (MOPs) (Coello Coello, 2006) are prevalent across diverse domains, including machine learning (Wang et al., 2019), bioinformatics (Bernardes et al., 2015), and scheduling (Sun et al., 2011). As the field expands and applications broaden, real-world MOPs exhibit growing complexity (Tian and Zhang, 2019), characterized by large-scale decision variables (Gu et al., 2024; Tian et al., 2021a), numerous objectives (Wu et al., 2025; Knowles and Corne, 2007), expensive evaluations (Luo et al., 2024), and intricate constraints (Neumann and Neumann, 2024; Liu et al., 2024).

To address various difficulties of complex MOPs, researchers designed different population-based multi-objective evolutionary algorithms (MOEAs) to tackle distinct complexities (Qian and Yu, 2017; Zille et al., 2018). However, this “one algorithm for one problem” paradigm often necessitates prior knowledge of problem characteristics and intricate algorithm design. To enhance MOEA generalization, recent work, inspired by pre-training successes in natural language processing (Brown et al., 2020; Ouyang et al., 2022) and computer vision (Dosovitskiy et al., 2021; Han et al., 2023), has explored pre-training for general-purpose optimization (Seiler et al., 2025; Li et al., 2024). Nevertheless, existing approaches predominantly focus on single-objective problems (Li et al., 2024) or small-scale decision spaces (Seiler et al., 2025), exhibiting poor scalability in both decision and objective spaces and consequently limited generalization to complex MOPs.

Taking this cue, we introduce a novel Population Pre-trained Model (PPM) for complex multi-objective optimization. *Conceptually*, PPM is pre-trained on solution pairs derived from existing methods across diverse MOPs to generate promising solutions. This model provides a learning-based alternative to traditional, stochastic reproduction operators like simulated binary crossover (SBX) (Deb et al., 1995), mutation (Storn and Price, 1997), and swarm particle update (Tian et al., 2020), leading to a new solution to improve the generalization of MOEAs. We provide a conceptual illustration for our idea in Figure 1.

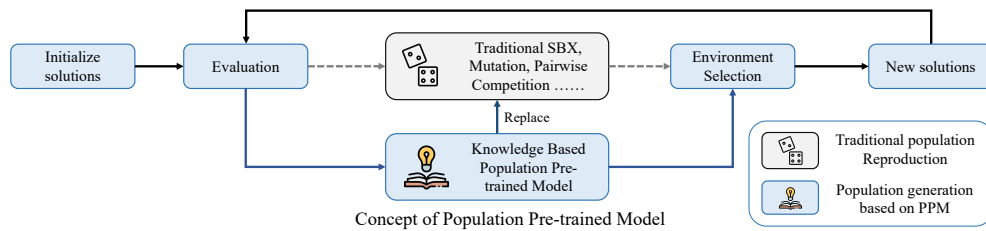


Figure 1: **Illustration of the proposed population pre-trained model.** Utilize PPM to solve complex MOPs (Initialization - Evaluation - Reproducing - Selection - Fine-tuning). PPM could be regarded as the replacement of the process of generating a new population, which generally contains SBX, mutation, particle update, etc.

Technically, we propose the population transformer based on the classical transformer architecture (Vaswani et al., 2017) to learn evolutionary knowledge from prior problems. Leveraging this, we introduce dimension embedding and objective fusion mechanisms to enhance the ability of our transformer to represent solutions with improved scalability and generalization across decision and objective spaces. First, di-

mension embedding maps problems with varying decision-space dimensionalities into a common latent space, enabling learning across scales and handling MOPs with up to 5,000 variables – five times the scale of the training problem and nearly 200 times greater than prior work Li et al. (2024). Second, objective fusion integrates objective features with decision features to capture interdependencies between decision variables and objective values during evolution. This allows the model to learn evolutionary knowledge of decision variables under multi-objective convergence and diversity pressure, predicting subsequent populations with improved performance. Our main contributions are:

1) This paper introduces a unified framework, the Population Pre-trained Model (PPM), for solving complex MOPs. Our model learns population-level patterns during evolution across diverse optimization problems, representing, to our knowledge, the first general-purpose solver for complex MOPs.

2) We demonstrate the efficacy of the PPM by introducing a specific population transformer architecture. To tackle the challenges of existing approaches in modeling diverse and high-dimensional decision spaces and capturing evolutionary information from objective values, this architecture incorporates two novel mechanisms: a dimension embedding mechanism to handle variable scales of decision variables, and an objective fusion mechanism to integrate objective information into the model training. These mechanisms ensure robust performance and generalization across complex MOPs of diverse scales.

3) Our population pre-trained model serves as a plugin module that can be integrated seamlessly into existing MOEAs, enhancing their ability to solve complex MOPs. Experimental results demonstrate state-of-the-art performance across diverse problem classes, including large-scale MOPs (up to 5,000 decision variables) (Tian et al., 2021b; Wang et al., 2021), many-objective problems (up to 10 objectives) (Li et al., 2015), computationally expensive problems (evaluated under a 1,000-function-evaluation budget) (Chugh et al., 2019), and real-world constrained MOPs (He et al., 2020).

The paper is structured as follows. Section 2 establishes multi-objective optimization notation and complex MOP classifications. Section 3 details the PPM framework and its implementation. Section 4 presents experimental validation and analysis, while Section 5 concludes with research contributions and future directions.

2 Preliminaries

This section provides a concise review of complex MOPs, their inherent challenges, and the corresponding MOEAs. Subsequently, we discuss recent advances of pre-trained models for optimization problems.

2.1 Complex MOPs and Corresponding MOEAs

Multi-objective optimization problems (MOPs) can be mathematically formulated as follows:

$$\begin{aligned} & \text{minimize } \mathbf{f}(\mathbf{x}) := (f_1(\mathbf{x}), f_2(\mathbf{x}), \dots, f_m(\mathbf{x})) \\ & \text{subject to } \mathbf{x} \in \Omega \end{aligned} \quad (1)$$

where $\mathbf{x} = (x_1, x_2, \dots, x_d)$ is d -dimensional decision vector, $\mathbf{f} = (f_1, f_2, \dots, f_m)$ is m -dimensional objective vector. Suppose \mathbf{x}_1 and \mathbf{x}_2 are two solutions of an MOP, solution \mathbf{x}_1 is known to Pareto dominate solution \mathbf{x}_2 (denoted as $\mathbf{x}_1 \prec \mathbf{x}_2$), if and only if $f_i(\mathbf{x}_1) \leq f_i(\mathbf{x}_2) (\forall i = 1, \dots, m)$ and there exists at least one objective $f_j (j \in \{1, 2, \dots, m\})$ satisfying $f_j(\mathbf{x}_1) < f_j(\mathbf{x}_2)$. The collection of all the Pareto optimal solutions in the decision

space is called the Pareto optimal set (PS), and the projection of PS in the objective space is called the Pareto optimal front (PF).

2.1.1 Complex MOPs

As research on MOPs advances, increasingly complex MOPs with different characteristics are being explored. These complex MOPs are frequently encountered in real-world scenarios. A notable example is the Transformation Ratio Error Estimation (TREE) problem (He et al., 2020), which necessitates the simultaneous consideration of computationally expensive evaluation functions, constraints, and large-scale decision variables. This subsection introduces properties including large-scale decision variables, many objectives, expensive evaluation functions, and constraints, along with existing MOEAs designed to address these challenges.

Large-scale Decision Variables. An MOP is classified as large-scale (LSMOP) when the number of decision variables $d \geq 100$ (Tian et al., 2021b; Wang et al., 2021). LSMOPs face the *curse of dimensionality* (Tian et al., 2021b; Hong et al., 2024), where computational difficulty grows exponentially with d , causing slow convergence in conventional algorithms. Recent MOEAs for LSMOPs fall into three categories: decision variable grouping-based (Antonio and Coello, 2013), decision space reduction-based (Zille et al., 2018), and novel search strategy-based approaches (He et al., 2022; Hong et al., 2022).

Many Objectives. An MOP becomes a many-objective optimization problem (MaOP) when objectives exceed three ($m > 3$) (Li et al., 2015). Increasing m challenges MOEAs through two effects: solution incomparability due to a rapidly rising proportion of non-dominated solutions (Knowles and Corne, 2007), and exponential growth in solutions needed to approximate high-dimensional Pareto fronts (Ishibuchi et al., 2015). Many-objective evolutionary algorithms (MaOEAs) are categorized into seven classes based on their techniques (Li et al., 2015), with detailed reviews available therein.

Expensive Evaluation Functions. MOPs with objectives requiring extensive computation time per evaluation are termed computationally expensive MOPs (EMOPs) (Chugh et al., 2019; Poloni et al., 2000). Surrogate models (e.g., Kriging, artificial neural networks, polynomial regression) are commonly integrated into MOEAs to approximate these functions (Pan et al., 2019), replacing costly exact evaluations.

Constrained Optimization. Constrained MOPs (CMOPs) incorporate constraints into Eq. (1) as $g_j(\mathbf{x}) \leq 0$ ($j = 1, \dots, l$) for inequalities and $h_j(\mathbf{x}) = 0$ ($j = l + 1, \dots, k$) for equalities, where l and $k - l$ denote inequality/equality constraint counts (Liang et al., 2023). Significant research focuses on constraint handling techniques (CHTs), driving the development of specialized constrained MOEAs (CMOEAs) (Liang et al., 2023).

Complex MOPs with Multiple Complexities. Beyond single complexities, real-world optimization problems generally show multiple complexities (He et al., 2020) and recent MOEAs target combined challenges like large-scale MaOPs (Deng et al., 2023), constrained large-scale MOPs (He et al., 2021; Ming et al., 2023), and expensive MaOPs (Habib et al., 2019). However, despite these advancements, the resolution of complex MOPs with more complexities, which encompass two or more of the complexities, continues to pose a significant challenge. For example, the exploration of expensive large-scale MOPs is largely uncharted due to the inefficiency of surrogate models such as Kriging (Emmerich et al., 2006) in learning the mapping between a multitude of decision variables and multiple objectives (Tian et al., 2021b). This gap motivates our universal framework for MOPs with diverse complexities.

2.2 Pre-trained Models in Optimization

Pre-trained Models. Pre-trained models encode visual (He et al., 2016; Dosovitskiy et al., 2021) or natural language (Brown et al., 2020) knowledge acquired from massive datasets. These models capture general patterns and semantic representations, serving as valuable resources for downstream tasks. For instance, pre-trained language models can solve diverse tasks previously requiring specialized models, including language translation, sentiment analysis, and question answering. This success motivates the development of pre-trained models for solving optimization problems.

Pre-training for Optimization. Recent work introduced the Pre-trained Optimization Model (POM) for zero-shot single-objective optimization (Li et al., 2024). POM concentrates on addressing the zero-shot optimization by leveraging knowledge gained from optimizing diverse tasks. Additionally, Deep-ELA (Seiler et al., 2025) targets single- and multi-objective continuous optimization. However, current methodologies are constrained by limited decision spaces and fail to incorporate objective space information. To address these limitations, we propose a novel framework that generalizes to higher-dimensional search spaces and integrates objective values to guide population generation. This approach enhances both convergence and diversity, resulting in a more general solver for complex multi-objective problems.

3 Population Pre-trained Model

The pre-training of our proposed Population Pre-trained Model relies on three foundational components: the dataset, the training objective, and the model architecture. Specifically, (1) the dataset comprises a curated collection of populations generated by diverse MOEAs across a broad spectrum of MOPs; (2) the training objective is to predict the subsequent generation of a population given its predecessor; and (3) the model architecture is a bespoke Population Transformer designed for this purpose.

This section first introduces the preparation of the pre-training dataset and the training objective, then outlines the design rationale and architecture details for the PPM, and finally details the implementation of integrating the PPM as a plugin into existing MOEAs.

3.1 Pre-training dataset and objective

To equip the Population Transformer Model with the capability to address Hull address complex MOPs, we pre-train it on a carefully curated dataset of populations generated by various MOEAs across diverse MOPs.

Dataset. As illustrated in Figure 2 (a), the dataset consists of paired populations from consecutive generations, thereby capturing the evolutionary dynamics inherent in diverse MOPs. These pairs are derived from outputs of established MOEAs applied to various MOPs, providing a rich collection of solution sets that reflect real-world optimization scenarios. The inclusion of multiple algorithms and problems in the dataset promotes robustness, enabling the model to generalize across different optimization problems and objective landscapes.

Training Objective. As depicted in Figure 2 (b), the pre-training objective of the PPM is to predict the population of the subsequent generation based on the current one. This predictive task mimics the iterative nature of evolutionary algorithms, training the model to anticipate improvements in solution quality over generations. Detailed

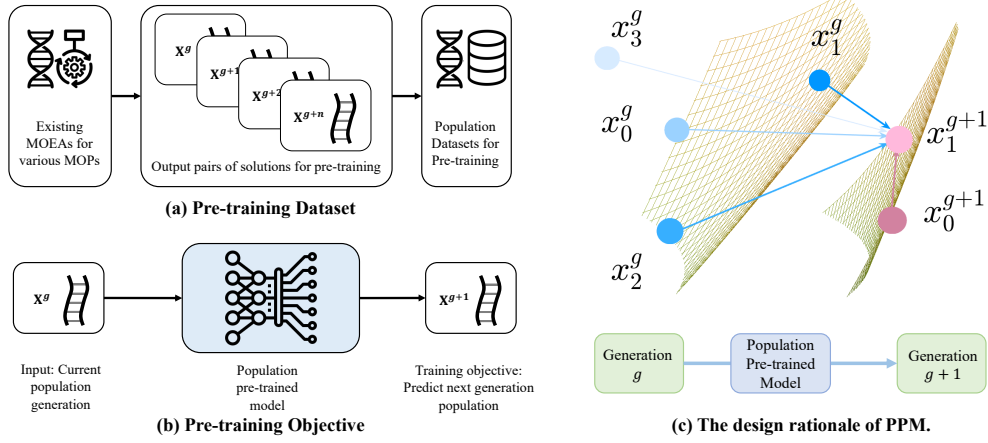


Figure 2: **Illustration of the proposed population pre-trained model: dataset, pre-training, and design rationale.** (a) The pre-training dataset is constructed from solution pairs generated by existing MOEAs across diverse MOPs. (b) The training objective of the PPM is to predict a next-generation population exhibiting better convergence and diversity, using the current population as input. (c) The figure illustrates the self-attention mechanism inherent in PPM. It stimulates the attention outcomes during the generation of the solution x_1^{g+1} . The color of the circle and line corresponds to the magnitude of the attention score, with darker shades indicating larger scores.

implementation aspects of the dataset curation and pre-training process are elaborated in the experimental section (Section 4.3).

3.2 Design Rationale of Population Transformer

Seq2Seq and Pop2Pop Adaptation. Transformer architectures inherently process sequential input to generate sequential output. Within heuristic MOEAs, populations represent sequences of solutions, and offspring generation relies on specialized operators. Consequently, adapting attention-based models to function as population-to-population (pop2pop) mappings is a natural progression.

Attention Mechanism. Transformers leverage self-attention within inputs and cross-attention between inputs and outputs. Analogously, the proposed PPM computes self-attention among solutions within a single generation and cross-attention between consecutive generations. By integrating objective-space information into solution representations and modeling attention across solutions, the quality of generated offspring is enhanced. Figure 2 (c) provides a simulated illustration of this attention mechanism within the PPM.

3.3 Architecture Details

To develop a Population Transformer capable of processing and generating promising solutions, we employ the classical Transformer architecture (Vaswani et al., 2017; Brown et al., 2020; Peebles and Xie, 2023).

As illustrated in Figure 3 (a), the complete population pre-trained model contains dimension embedding (component 1), objective fusion (component 2), and population transformer architecture (component 3). These components enable the transformer to

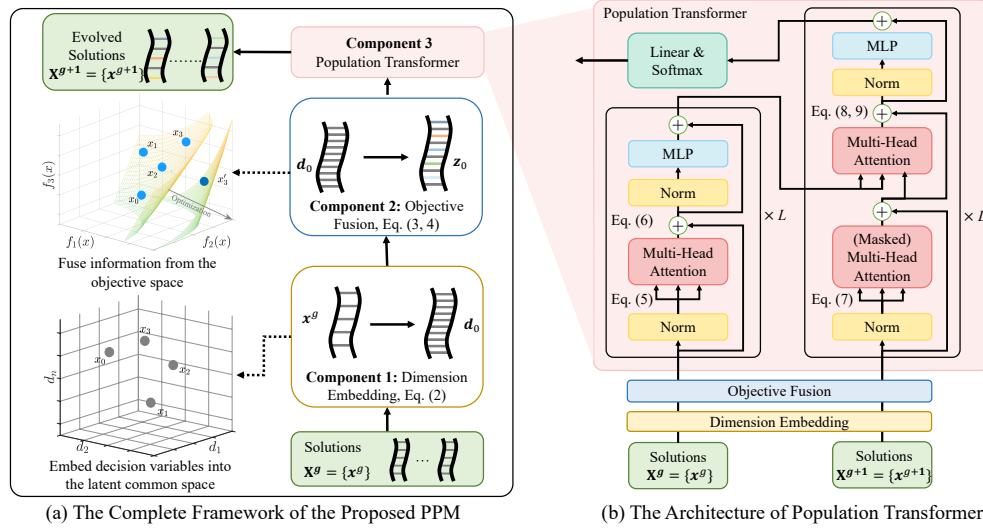


Figure 3: (a) The framework of the proposed Population Transformer, an instantiation of PPM, operates as follows: 1. Collect the population $\mathbf{X}^g = \mathbf{x}^g$ at generation g . 2. Embed the decision variable dimensions of \mathbf{x}^g using Eq. (2) to obtain \mathbf{d}_0 . 3. Fuse objective values into \mathbf{d}_0 via Eq. (3) and (4) to obtain \mathbf{Z}_0 . 4. Process \mathbf{Z}_0 using the PPM. 5. Output the next-generation population $\mathbf{X}^{g+1} = \mathbf{x}^{g+1}$. (b) The architecture of the population transformer. During pre-training, $\mathbf{X}^{g+1} = \{\mathbf{x}^{g+1}\}$ are target solutions but masked for training. During fine-tuning, $\mathbf{X}^{g+1} = \{\mathbf{x}^{g+1}\}$ are generated solutions by PPM, and once one solution \mathbf{x}^{g+1} is generated, \mathbf{x}^{g+1} will be evaluated and then input to the PPM.

process populations with varying dimensionalities and generate subsequent population states, guided by convergence and diversity information derived from objective spaces.

3.3.1 Dimension Embedding

The dimensionality of solutions varies across different MOPs. This variation complicates learning population representations from disparate decision spaces and limits the generalization capability of existing methods to high-dimensional problems. To address this, we propose dimension embedding. This technique projects solutions from diverse dimensional spaces into a higher-dimensional, common latent space, enabling the population transformer to handle MOPs with varying decision variable scales and generalize effectively to high-dimensional MOPs.

The standard transformer requires fixed-size token embeddings. To process variable-dimensional solutions, we first pad each solution $\mathbf{X}^g = \{\mathbf{x}_0^g, \dots, \mathbf{x}_N^g\}$ (where $\mathbf{x}_i^g \in \mathbb{R}^d$) in generation g with zeros to a uniform dimension \hat{d} . Subsequently, these padded solutions, originating from diverse problems and decision spaces, are projected into a common latent space via a trainable linear transformation following the standard token embedding method. This linear transformation is implemented using a multi-layer perceptron, mapping \mathbf{X}^g to a set of latent vectors $\mathbf{D}_0^g = \{\mathbf{d}_0^g, \dots, \mathbf{d}_N^g\}$ ($\mathbf{d}_i^g \in \mathbb{R}^{d'}$). Here, d' denotes the predefined input size of the PPM, corresponding to the maximum dimension it can process. We term \mathbf{D}_0^g the “solution embeddings”.

The PPM processes the entire population of n solutions concurrently within a generation. This population size n also defines the effective input sequence length for the transformer. The dimension embedding ensures the generalization across different de-

cision spaces within d' and is denoted by:

$$\mathbf{D}_0^g = [\mathbf{x}_0^g \mathbf{E}_{\text{dim}}; \mathbf{x}_1^g \mathbf{E}_{\text{dim}}; \cdots \mathbf{x}_N^g \mathbf{E}_{\text{dim}}], \mathbf{E}_{\text{dim}} \in \mathbb{R}^{d \times d'}, \quad (2)$$

where \mathbf{E}_{dim} is the learnable linear projection.

3.3.2 Objective Fusion

The evaluation of solutions plays a crucial role in the evolving process of MOEAs. To enhance the learning capabilities of the proposed model in capturing solution evolution to output promising solutions, it is essential to incorporate the evaluation into the solution. Moreover, it is important to note that the proximity of two solutions in the decision space does not necessarily imply similarity in the objective space. Therefore, integrating evaluation information into the solution representation is important to capture relationships between objectives and improve the quality of evolved solutions.

In this regard, objective fusion is introduced to integrate evaluation information into the solution representation. By embedding the positions of solutions within the objective space, the model can better capture relationships between objectives and improve the quality of evolved solutions. With this approach, we combine the position of the solution in the objective space into solution embeddings \mathbf{D}_0^g , enabling the integration of evaluation information into the PPM.

We use standard learnable position embeddings to obtain objective embeddings \mathbf{O}_0^g in Eq. (3). Afterward, objective embeddings are added to the solution embeddings to retain positional information in the objective space, and the resulting sequence of embedding vectors \mathbf{Z}_0^g (Eq. (4)) serves as input to the encoder of the population transformer.

$$\mathbf{O}_0^g = [\mathbf{f}_0^g \mathbf{E}_{\text{obj}}; \mathbf{f}_1^g \mathbf{E}_{\text{obj}}; \cdots \mathbf{f}_N^g \mathbf{E}_{\text{obj}}], \mathbf{E}_{\text{obj}} \in \mathbb{R}^{m \times d'}, \quad (3)$$

$$\mathbf{Z}_0^g = \mathbf{D}_0^g + \mathbf{O}_0^g, \quad (4)$$

where \mathbf{f}_i^g is i -th objective value of solution g and \mathbf{E}_{obj} is the learnable linear projection.

3.3.3 Population Transformer

As the PPM is designed to generate next-generation promising solutions, a Transformer with an encoder-decoder architecture is employed (Vaswani et al., 2017). Both the encoder and decoder comprise a stack of N identical layers (where $N = L$). As illustrated in Figure 3 (b), the model follows an auto-regressive approach (Graves, 2013), utilizing stacked self-attention and fully connected layers in both components.

Encoder. The encoder receives \mathbf{Z}_0^g as the input and maps to a sequence of continuous representations \mathbf{Z}_L^g . The encoder consists of layers of Multi-Headed Attention (MHA) and Multilayer Perceptron (MLP) blocks, and layer norm (LN) is applied before every block and residual connections after every block (Eq. (5, 6)).

$$\mathbf{Z}_{l+1}^g = \text{MHA}(\text{LN}(\mathbf{Z}_l^g)) + \mathbf{Z}_l^g \quad (5)$$

$$\mathbf{Z}_{l+1}^g = \text{MLP}(\text{LN}(\mathbf{Z}_{l+1}^g)) + \mathbf{Z}_{l+1}^g \quad (6)$$

$$l = 0, \dots, L - 1.$$

Decoder. After fusing \mathbf{X}^g into \mathbf{Z}_L^g , the decoder then generates one next generation ($g + 1$) of solution \mathbf{x}^{g+1} at a time. At each step, the model consumes the previously generated solutions as additional input when generating the next.

Given the newly generated solutions x_n^{g+1} and accumulated solutions \mathbf{X}^{g+1} , to generate the next x_{n+1}^{g+1} , the PPM firstly evaluates the x_n^{g+1} and obtain its objective f . Second, the decoder receives \mathbf{X}^{g+1} (including x_n^{g+1}) as the input for dimension embedding and objective fusion and obtains \mathbf{Z}_0^{g+1} . Third, the decoder processes \mathbf{Z}_0^{g+1} through LN and MHA via Eq. (7) to obtain \mathbf{Z}_L^{g+1} .

After obtaining \mathbf{Z}_{l+1}^g and \mathbf{Z}_{l+1}^{g+1} , the decoder employs the attention mechanism, which allows it to focus on relevant parts of the input solutions by computing a weighted sum of values based on the similarity between query and key vectors. Specifically, the attention mechanism calculates the cross-attention \mathbf{C}_{l+1}^{g+1} by using the output of the previous decoder block (\mathbf{Z}_{l+1}^{g+1}) as the query \mathbf{Q} , and the encoder's output (\mathbf{Z}_{l+1}^g) as the key \mathbf{K} and value \mathbf{V} (Eq. (8)). This procedure is essentially an aggregation of the information from the whole solutions at generation g and generated solutions at generation $g + 1$.

Finally, the decoder applies residual connections to the cross attention \mathbf{C}_{l+1}^{g+1} and \mathbf{Z}_{l+1}^{g+1} and input the result to the MLP after layer norm (Eq. (9)). The masked MHA block of the decoder ensures that the generation for solution x_n^{g+1} can depend only on the known solutions before n .

$$\mathbf{Z}_{l+1}^{g+1} = \text{MHA}(\text{LN}(\mathbf{Z}_l^{g+1})) + \mathbf{Z}_l^{g+1} \quad (7)$$

$$\mathbf{C}_{l+1}^{g+1} = \text{MHA}(\mathbf{Z}_{l+1}^g(\mathbf{K}, \mathbf{V}), \mathbf{Z}_{l+1}^{g+1}(\mathbf{Q})) \quad (8)$$

$$\mathbf{Z}_{l+1}^{g+1} = \text{MLP}(\text{LN}(\mathbf{C}_{l+1}^{g+1} + \mathbf{Z}_{l+1}^{g+1})) + \mathbf{C}_{l+1}^{g+1} \quad (9)$$

$$l = 0, \dots, L - 1$$

The final output (\mathbf{Z}_L^{g+1}) of the decoder goes through the linear layer and the softmax layer, and finally, the $(n + 1)$ th solution of the $(g + 1)$ th generation is obtained.

3.4 Method Modularity and Its Implementation

Once the pre-trained PPM has been acquired, it can be integrated into any MOEAs to solve other complex MOPs. The PPM serves as a replacement for the conventional method of generating the next generation of solutions. Algorithm 1 provides an example algorithm that combines PPM with the NSGA-II (Deb et al., 2002). Specifically, the "fast-non-dominated-sort" and "crowding-distance-selection" steps in this algorithm refer to the environmental selection process of NSGA-II. Instead of utilizing crossover and mutation operators, the creation of new populations is accomplished by $\mathbf{X}^{g+1}, \mathbf{F}^{g+1} \leftarrow \text{PPM}(\mathbf{X}^g, \mathbf{F})$, leveraging the proposed pre-trained PPM.

In addition to NSGA-II, the proposed PPM can collaborate with any available MOEA to harness pre-trained knowledge and facilitate the generation of improved populations, resulting in faster convergence to the Pareto frontier. At the g th iteration of any MOEA, PPM receives the solutions \mathbf{X}^g and their corresponding evaluations, which are then passed as inputs to the encoder of PPM. During the generation process, the decoder of PPM initializes the $(g + 1)$ -th generation by accepting a randomly selected solution as the initialization token. Subsequently, PPM generates a solution for the $(g + 1)$ -th generation, evaluates it, and feeds it back into the decoder for further refinement. Ultimately, PPM delivers the complete population of the $(g + 1)$ -th generation, denoted as \mathbf{X}_{g+1} , to the cooperative MOEA.

The core idea of the proposed method is to learn evolutionary patterns between generations from existing algorithms, thereby enabling the model to generate promis-

Algorithm 1 NSGA-II with PPM**Input:** P : PPM.**Parameter:** N : Population size, E : Total function evaluations.**Output:** \mathbf{X}^G : Output solutions.

```

1: Initialize a set of  $N$  solutions  $\mathbf{X}^0$ ;
2:  $\mathbf{F}^0 \leftarrow \text{Evaluate}(\mathbf{X}^0)$ ;
3:  $E \leftarrow E - N$ ;
4: while  $E > 0$  do
5:    $\mathcal{F} \leftarrow \text{fast-non-dominated-sort}(\mathbf{X}^g, \mathbf{F}^g)$ ;
6:    $\mathbf{X}^g \leftarrow \text{crowding-distance-selection}(\mathcal{F})$ ;
7:    $\mathbf{X}^{g+1}, \mathbf{F}^{g+1} \leftarrow \text{PPM}(\mathbf{X}^g, \mathbf{F})$ ;
8:    $\text{PPM} \leftarrow \text{fine-tune}(\text{PPM}, \mathbf{X}^g, \mathbf{F}, \mathbf{X}^{g+1}, \mathbf{F}^{g+1})$ ;
9:    $E \leftarrow E - N$ ;
10:   $g \leftarrow g + 1$ ;
11: end while
12: return  $\mathbf{X}^G$ 

```

ing solutions for new complex MOPs. The effectiveness of the proposed model is verified through extensive experiments, as discussed in the subsequent section.

4 Experiments

In this section, we first outline the experimental settings used for comparison. We then evaluate the performance of the proposed PPM in addressing complex MOPs, which include large-scale decision variables, many objectives, expensive evaluation functions, and constraints. The experiments are conducted on a variety of benchmarks, including real-world problems. Finally, we present an ablation study and analyze the convergence and computational efficiency of the proposed method.

4.1 Experimental Setup

Compared Algorithms. NSGA-II (Deb et al., 2002) is used as the baseline as it is used for our specific implementation. Besides, we choose SOTA methods that are specialized in solving large-scale, many objective, constrained, and expensive MOPs: CCGDE3 (Antonio and Coello, 2013) and WOF (Zille et al., 2018) are algorithms for solving LSMOPs, LMOCSSO (Tian et al., 2020) can solve MOP efficiently (Zille et al., 2018), DGEA (He et al., 2022) has advantages in solving LSMOPs and MaMOPs (He et al., 2022), and CMOEAD (Deb and Jain, 2014) is designed for MOPs with constraints. CMOCSSO (Ming et al., 2023) are designed for solving large-scale constrained MOPs. POCEA (He et al., 2021) shows promising performance in solving large-scale constrained MaOPs. Besides, we include two machine learning-based MOEAs, EmoDM (Yan and Jin, 2024) and MODE/D-LO (Liu et al., 2023), for comparison. They utilize the diffusion model and a large language model to search for better solutions, respectively.

Parameter Setting. General parameters and algorithm parameters are presented as follows:

1. Population Size. To ensure consistency across all test benchmarks, the population size is set to 100 (Tian et al., 2020; He et al., 2022).
2. Termination Condition. To test the performance of algorithms on expensive optimization problems, the number of maximum evaluations E is set to 1,000 for all

Table 1: Parameters for The Proposed PPM.

Dim embed size d'	Batch size	Layers	Hidden size D	Heads
10,000	64	11	512	10
Optimizer	beta1	beta2	Weight decay	# Parameters
Adam (Kingma and Ba, 2015)	0.9	0.999	0.1	61M

compared MOEAs (Chugh et al., 2019).

3. Algorithm Parameters. Parameters for the PPM are listed in Table 1. All algorithms are implemented in PlatEMO (Tian et al., 2017), and the parameter settings for all compared algorithms follow their original publications to ensure fair comparison. The parameter settings for each algorithm are detailed in Table 8 in Appendix B.

Benchmarks. The experiments utilize three widely adopted benchmark suites: ZDT (Zitzler et al., 2000), LSMOP (Cheng et al., 2017), and TREE (He et al., 2020). The ZDT suite is commonly used to test the scalability of algorithms with respect to different Pareto front shapes and solution complexities. The test problem suite LSMOP (Cheng et al., 2017) is commonly employed for evaluating the performance of MOEAs in the presence of decision variables and objectives that scale differently. Lastly, the TREE problem represents a real-world constrained MOP, allowing us to assess how well the algorithms handle practical optimization challenges with strict constraints and computationally expensive objective functions. Specifically, TREE (He et al., 2020) is an important real-world task in modern power delivery systems, which aims to detect the voltage transformers' ratio error (RE). Based on the statistical and physical rules, the TREE is modeled as several computationally expensive, constrained, large-scale MOPs. Objectives include total time-varying, the sum of the RE variation, and the phase angle relationship among the true voltage values. Constraints contain topology, series, and phase constraints.

4.2 Metrics

We employ the Inverted Generational Distance (IGD) (Zitzler et al., 2003) and Hypervolume (HV) (While et al., 2006) metrics to rigorously assess the convergence and diversity of algorithms addressing complex MOPs. The IGD metric quantifies the convergence quality of solutions by measuring the average distance from a reference set to the obtained solutions, with lower values indicating superior convergence performance. The HV metric evaluates the diversity and dominance of a solution set by calculating the volume of the objective space collectively dominated by those solutions, where a larger HV signifies better overall performance.

Each algorithm is run 20 times independently, and the Wilcoxon rank-sum (Haynes, 2013) is used to compare the statistical results obtained at a significance level of 0.05. In the tables, (+/-/=) indicate that compared algorithms perform significantly better, significantly worse, or indifferent compared to the PPM, respectively, in a statistically meaningful sense.

4.3 Pre-Training

To evaluate the performance of the pre-training stage, we conducted experiments on the ZDT and LSMOP benchmark problems using NSGA-II, DGEA, and WOF. These algorithms were chosen because of their proven ability to explore and exploit solution

Table 2: IGD Values Obtained by Compared Algorithms on 16 Instances From ZDT and LSMOP Test Suite. The Best Result in Each Row is Highlighted in Bold. The Last Column Represents the Rate of Change of the Proposed PPM Compared to Suboptimal Results.

Problem	D	NSGA-II	CCGDE3	DGEA	WOF	LMOCSSO	CMOEA	POCEA	CMOCSSO	ABSAEA	CSEA	EmoDM	MOEA/D-LO	PPM	ROC(%)
ZDT6 M=2	250	7.48e+00	7.63e+00	7.62e+00	7.67e+00	7.50e+00	7.66e+00	7.69e+00	7.47e+00	7.69e+00	7.76e+00	7.72e+00	7.70e+00	6.55e-01	91.23
	2500	7.79e+00	7.81e+00	7.84e+00	7.80e+00	7.85e+00	7.86e+00	7.84e+00	7.72e+00	7.83e+00	7.87e+00	6.15e+01	9.08e+04	6.55e-01	91.52
	3000	7.78e+00	7.85e+00	7.84e+00	7.79e+00	7.85e+00	7.86e+00	7.85e+00	7.80e+00	7.83e+00	7.87e+00	6.06e+01	2.11e+01	6.55e-01	91.58
	5000	7.83e+00	7.86e+00	7.85e+00	7.83e+00	7.83e+00	7.90e+00	7.87e+00	7.82e+00	4.55e+01	4.55e+01	4.55e+01	6.12e+01	6.55e-01	91.62
LSMOP7 M=2	250	4.41e+04	3.74e+04	2.12e+04	5.55e+04	3.72e+03	4.17e+04	3.31e+03	3.04e+04	6.47e+04	8.53e+04	7.72e+00	7.75e+00	1.50e+00	80.58
	2500	8.24e+04	8.06e+04	1.17e+04	7.95e+04	1.01e+04	8.13e+04	3.90e+03	3.50e+04	8.39e+04	9.05e+04	9.00e+04	9.19e+04	1.52e+00	99.96
	3000	8.00e+04	7.13e+04	2.61e+04	8.32e+04	6.73e+03	8.48e+04	4.70e+03	2.40e+04	8.50e+04	9.36e+04	6.06e+01	2.11e+01	1.52e+00	92.79
	5000	8.62e+04	8.03e+04	9.30e+03	8.59e+04	9.51e+03	8.45e+04	5.47e+03	2.26e+04	4.55e+01	4.55e+01	4.55e+01	6.12e+01	1.52e+00	96.66
LSMOP8 M=2	250	1.32e+01	1.62e+01	6.96e+00	3.69e+00	5.03e+00	1.55e+01	3.36e+00	9.82e+00	1.77e+01	1.88e+01	7.72e+00	7.75e+00	7.42e-01	77.91
	2500	1.92e+01	1.85e+01	7.78e+00	1.94e+01	5.99e+00	1.99e+01	3.86e+00	8.58e+00	1.96e+01	2.11e+01	9.08e+04	9.19e+04	7.42e-01	80.79
	3000	1.89e+01	1.85e+01	8.99e+00	4.63e+00	7.39e+00	2.03e+01	4.18e+00	8.74e+00	2.00e+01	2.07e+01	2.09e+01	2.04e+01	7.42e-01	82.24
	5000	2.03e+01	1.81e+01	1.35e+01	2.11e+01	6.78e+00	2.10e+01	4.20e+00	8.38e+00	4.55e+01	4.55e+01	4.55e+01	6.12e+01	7.42e-01	82.33
LSMOP9 M=2	250	3.67e+01	4.08e+01	4.83e+01	4.17e+01	2.15e+01	3.09e+01	6.73e+00	2.89e+01	3.81e+01	5.26e+01	7.72e+00	7.75e+00	8.10e-01	87.96
	2500	5.70e+01	5.45e+01	4.21e+01	5.43e+01	3.15e+01	5.49e+01	1.73e+01	4.06e+01	5.70e+01	6.15e+01	9.08e+04	9.19e+04	8.10e-01	95.31
	3000	5.54e+01	5.42e+01	4.22e+01	6.11e+01	1.69e+01	5.55e+01	7.12e+00	4.29e+01	5.73e+01	6.06e+01	2.11e+01	2.04e+01	8.10e-01	88.63
	5000	5.80e+01	5.53e+01	4.71e+01	1.25e+01	2.88e+01	5.82e+01	1.24e+01	4.50e+01	4.55e+01	4.55e+01	6.10e+01	6.08e+01	8.10e-01	93.44
(+/-/=)		0/16/0	0/16/0	0/16/0	0/16/0	0/16/0	0/16/0	0/16/0	0/16/0	0/16/0	0/16/0	0/16/0	0/16/0		

Table 3: HV Values Obtained by Compared Algorithms on 36 Instances From LSMOP Test Suite. The Best Result in Each Row is Highlighted in Bold. The Last Column Represents the Rate of Change of the Proposed PPM Compared to Suboptimal Results.

Problem	D	NSGAII	CCGDE3	DGEA	WOF	LMOCSSO	CMOEA	POCEA	CMOCSSO	ABSAEA	CSEA	EmoDM	MODE/D-LO	PPM	ROC (%)
ZDT6 M=2	250	0.00e+00	0.00e+00	0.00e+00	0.00e+00	0.00e+00	8.15e-02	5.95e-02	7.00e-02	6.95e-02	6.17e-02	0.00e+00	6.63e-02	1.91E-01	11.53
	2500	0.00e+00	0.00e+00	2.13e-02	0.00e+00	1.64e-02	0.00e+00	8.65e-02	3.69e-02	6.28e-02	0.00e+00	0.00e+00	8.47e-02	9.01E-02	5.09
	3000	0.00e+00	0.00e+00	3.03e-02	1.66e-02	0.00e+00	0.00e+00	8.00e-02	5.84e-02	0.00e+00	0.00e+00	0.00e+00	0.00e+00	7.09E-02	55.65
	5000	0.00e+00	0.00e+00	0.00e+00	6.99e-03	6.69e-03	0.00e+00	8.64e-02	5.23e-02	4.86e-02	0.00e+00	3.02e-02	0.00e+00	8.09E-02	5.21
LSMOP7 M=2	250	0.00e+00	0.00e+00	0.00e+00	4.79E-03+	6.77e-02+	7.06e-02+	6.65e-02+	0.00e+00	0.00e+00	0.00e+00	1.13e-02+	0.00e+00	0.00e+00	-100.00
	2500	0.00e+00	0.00e+00	1.87e-03+	0.00e+00	3.40e-02+	3.77e-02+	1.79e-02+	8.84e-02+	3.00e-02+	0.00e+00	5.33e-02+	0.00e+00	0.00e+00	-100.00
	3000	0.00e+00	0.00e+00	7.91e-02+	4.18e-02+	7.88e-02+	3.28e-02+	7.94e-02+	6.59e-02+	8.80e-02+	7.63e-02+	0.00e+00	0.00e+00	0.00e+00	-100.00
	5000	0.00e+00	0.00e+00	2.80e-02+	0.00e+00	0.00e+00	7.86e-02+	8.70e-02+	0.00e+00	0.00e+00	0.00e+00	4.70e-02+	4.67e-02+	0.00e+00	-100.00
LSMOP8 M=2	250	0.00e+00	0.00e+00	0.00e+00	0.00e+00	0.00e+00	6.94e-02	0.00e+00	0.00e+00	2.64e-02	6.04e-02	6.86e-02	4.11e-02	9.09E-02	30.98
	2500	0.00e+00	0.00e+00	4.27e-02	0.00e+00	0.00e+00	1.70e-02	7.30e-02	0.00e+00	0.00e+00	0.00e+00	6.26e-02	4.91e-02	9.09E-02	24.52
	3000	0.00e+00	0.00e+00	4.37e-02	0.00e+00	3.43e-04	1.98e-02	6.89e-02	0.00e+00	0.00e+00	2.53e-02	0.00e+00	0.00e+00	9.09E-02	31.93
	5000	0.00e+00	0.00e+00	2.55e-02	0.00e+00	0.00e+00	3.84e-02	0.00e+00	0.00e+00	0.00e+00	0.00e+00	1.41e-02	3.94e-02	9.09E-02	136.72
LSMOP9 M=2	250	0.00e+00	0.00e+00	0.00e+00	0.00e+00	4.85e-02	0.00e+00	5.39e-02	0.00e+00	0.00e+00	5.78e-02	3.85e-02	3.39e-02	9.09E-02	57.27
	2500	0.00e+00	0.00e+00	1.76e-02	0.00e+00	7.17e-02	5.60e-02	1.35e-02	0.00e+00	0.00e+00	4.23e-02	1.95e-03	3.65e-02	9.09E-02	26.78
	3000	0.00e+00	0.00e+00	0.00e+00	0.00e+00	0.00e+00	0.00e+00	6.62e-02	2.23e-02	0.00e+00	2.05e-02	0.00e+00	0.00e+00	9.09E-02	37.31
	5000	0.00e+00	0.00e+00	2.21e-02	2.91e-02	4.99e-02	0.00e+00	0.00e+00	8.75e-02	4.71e-03	0.00e+00	4.35e-02	0.00e+00	9.09E-02	3.89
(+/-/=)		0/12/4	0/12/4	3/12/1	2/12/2	3/12/1	4/12/0	4/12/0	2/12/2	1/12/3	3/12/1	1/12/3			

spaces effectively. The goal of pre-training is to train the proposed PPM on a diverse set of MOPs to generate high-quality populations. Specifically, we executed NSGA-II, DGEA, and WOF on ZDT 1-5 and LSMOP 1-6, performing $1,000 \times d$ function evaluations for each. We varied the number of decision variables d , setting them as 100, 200, 500, and 1,000, while the number of objectives was set to 2 and 3.

Throughout the runs, we recorded the populations at each generation. Considering generation g and generation $g + 1$ as a pair of populations for pre-training, PPM was utilized to generate a new population g' based on the input of population g , followed by the calculation of the loss between populations g' and $g + 1$. The pre-training process using PPM, performed on one A40 GPU with a Platinum 8358P CPU, required approximately two days for 1000 epochs.

4.4 Performance on Benchmarks

4.4.1 Experimental Results on Large-scale MOPs

We evaluated the generalization performance of the PPM on various problems, including ZDT and LSMOP. The obtained IGD values and HV values for all competing algorithms are presented in Table 2 and Table 3, respectively. We tested on ZDT6 and LSMOP7-9, which are different from the training problems, and scaled the dimension up to 5,000.

Table 2 reveals that PPM exhibits notable advantages in solving ZDT 6 with di-

mensions ranging from 250 to 5,000. Compared to the suboptimal algorithm, PPM showcases a remarkable improvement of 91%. Conversely, most of the compared algorithms show worse performance. In particular, AB-SAEA (Wang et al., 2020) and CSEA (Pan et al., 2019) fail to produce solutions even at dimension scales of 100 and 5,000. This observation validates the limitations of existing surrogate models in capturing the complex mapping between numerous decision variables and multiple objective functions (Tian et al., 2021b).

Table 3 showcases the algorithm’s performance in terms of HV. Notably, while all algorithms, including PPM, yield zero HV values for the LSMOP7 problem, the proposed algorithm achieves non-zero HV values for ZDT6, LSMOP8, and LSMOP9, outperforming the compared algorithms. This outcome demonstrates PPM’s superior performance compared to other algorithms. The HV values attained by PPM remain relatively consistent, primarily due to the limited number of solutions that approximate the Pareto front. Although this suggests that PPM may not exhibit perfect diversity, it is worth noting that it still outperforms existing algorithms.

4.4.2 Experimental Results on Large-scale MaOPs

We further expand the complexity of complex MOPs, and we present the IGD and HV values obtained by all algorithms in solving expensive, large-scale, many-objective optimization problems in Tables 4 and 5. The tested problem is scaled up to ten objectives.

The results show that there are advantages in many-objective (up to 10 objectives), large-scale decision variables (250-5,000 dimensions), and computationally expensive functions (only 1,000 function evaluations). Table 4 shows that the proposed PPM significantly outperforms compared algorithms on computationally expensive large-scale many-objective optimization problems (2,500 decision variables with 10 objectives and 1,000 function evaluations). We noticed that WOF, CMOEAD, and MOEA/D-LO achieved several of the best results with the IGD indicator, but their overall performance is still unsatisfactory.

Although LSMOP 1-9 is a series of test sets, different test functions under this series have different properties. For example, different problems have different landscapes and their decision variables also have different separability (Cheng et al., 2017), while PPM can utilize learned patterns on evolutionary computation on LSMOP 1-6 and fine-tuning on LSMOP 7-9 problems, achieving superior results, which shows that the pre-training and fine-tuning are a valid paradigm in solving complex MOPs.

4.4.3 Visualization of Performance

Figure 4 depicts the non-dominated solutions obtained by different algorithms, with points of different colors, and the PF is located in the lower right corner of the figure. The first row of the figure displays all the solutions obtained by all the algorithms, while the second row provides an enlarged view near the PF to enhance visualization. The visual results align with the quantitative results and indicate that, despite some limitations in diversity, the proposed PPM excels at generating solutions that approximate the PF.

4.4.4 Experimental Results on Unseen Large-scale MOPs: LSMOP*

We further evaluated the generalization performance to LSMOP* benchmark (Gu et al., 2023), a variant of the original LSMOP benchmark that incorporates a translation transformation. Quantitative and visualization results are presented in Appendix D and E. The results show that our PPM also achieves the best performance when MOPs are different from the training problems.

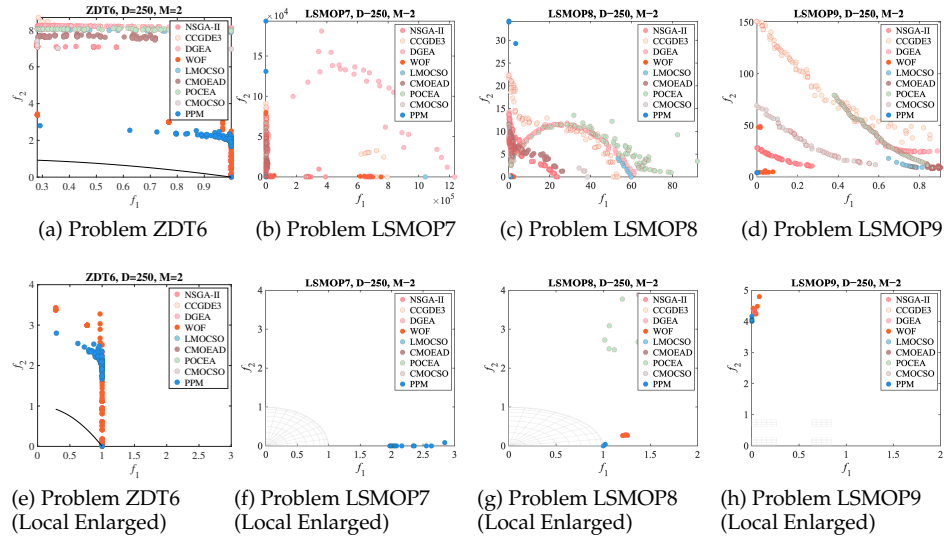


Figure 4: Visualization of Non-dominated Solutions Obtained by Each Algorithms on LSMOP7, LSMOP8, and LSMOP9. The first row of the Figures is the visualization of the complete solutions, and the second row is the scaled near PF for better visualization.

Table 6: IGD Values Obtained By Compared Algorithms on Real World Test Suite, TREE. The Best Result in Each Row is Highlighted in Bold. The Last Column Represents the Rate of Change of the Proposed PPM Compared to Suboptimal Results.

Problem	D	NSGA-II	CCGDE3	DGEA	WOF	LMOCSSO	CMOEAD	POCEA	CMOCSSO	PPM	ROC(%)
TREE1	3000	NaN+	NaN+	9.58e+01-	9.65e+01-	NaN+	NaN+	NaN+	NaN+	1.65e+00	98.28%
TREE2	3000	NaN+	NaN+	3.69e+02-	3.99e+02-	NaN+	NaN+	NaN+	NaN+	2.55e+02	30.90%
TREE3	6000	NaN+	NaN+	1.20e+02-	1.20e+02-	NaN+	NaN+	NaN+	NaN+	2.77e+01	76.87%
TREE4	6000	NaN+	NaN+	1.20e+02-	1.19e+02-	NaN+	NaN+	NaN+	NaN+	5.69e+01	52.10%
TREE5	6000	NaN+	NaN+	1.84e+02-	NaN+	NaN+	NaN+	NaN+	NaN+	1.02e+02	44.54%
(+/-/=)		0/5/0	0/5/0	0/5/0	1/4/0	0/5/0	0/5/0	0/5/0	0/5/0		

4.5 Performance Generalization to Real-world Applications

In addition to the pre-trained test problems ZDT and LSMOP, we also evaluate our algorithm on the TREE test problem, which aims to estimate the state of voltage transformers in real time. The TREE test set, with its large-scale nature (3,000 dimensions) and constraints, presents a more complex scenario compared to ZDT and LSMOP. The combination of large-scale decision variables, costly function evaluation, and constraints results in a vast search space. The available evaluations are strictly limited, and the solutions found may not necessarily be feasible, making it challenging for the algorithm to locate the PF or even feasible solutions.

Notably, the results presented in Table 6 indicate that our proposed PPM model significantly outperforms compared algorithms on the TREE test set. Despite the triple challenges of large-scale decision variables, expensive function evaluation, and constraints, our algorithm delivers the best results on TREE 1-5. In contrast, some algorithms fail to obtain feasible results. The tests on the TREE test set demonstrate that the proposed PPM can not only achieve impressive optimization results on real-world MOPs but also exhibit potential emergent abilities on some non-pre-trained problems.

Table 7: Ablation Study: IGD Values Obtained by Compared Algorithms and Untrained PPM.

Problem	D	M	NSGA-II	+PPM* [†]	WOF	+PPM* [†]
ZDT1	150	2	2.44e+00-	8.40e-01	1.88e+00+	2.37E+00
ZDT1	550	2	2.67e+00-	8.40e-01	2.54e+00=	2.57E+00
LSMOP1	150	2	7.18e+00-	7.07e-01	5.26e+00-	2.09e+00
LSMOP1	150	10	NaN+	NaN	NaN+	NaN
LSMOP1	550	2	1.05e+01-	7.07e-01	2.37e+00+	8.53E+00
LSMOP1	550	10	8.82e+00-	1.02e+00	8.56e+00=	8.53e+00
LSMOP2	150	2	1.99e-01+	6.39E-01	1.94e-01=	1.95E-01
LSMOP2	150	10	NaN+	NaN	NaN+	NaN
LSMOP2	550	2	6.76e-02+	7.07E-01	6.77e-02=	6.73e-02
LSMOP2	550	10	4.56e-01+	9.79E-01	4.03e-01+	5.01E-01

[†] +PPM* denotes embedding PPM into the NSGA-II and WOF without pre-training on any benchmarks. The untrained population transformer is used to generate new solutions for NSGA-II and WOF to validate the effectiveness of the pre-training in solving MOPs.

4.6 Ablation Study

This section examines the efficacy of pre-training. The untrained PPM was integrated into NSGA-II and WOF, replacing the offspring reproduction operators. The outcomes are presented in Table 7. The experimental findings suggest that the untrained PPM is largely ineffective in resolving complex MOPs. The performance of the untrained PPM in population generation resembles the original reproduction operators of NSGA-II and WOF, which are essentially stochastic generating. This further illustrates the effectiveness of pre-training and fine-tuning in generating better solutions to solve complex MOPs.

4.7 Convergence and Computational Efficiency

The progression of IGD values for all compared algorithms on the ZDT6, LSMOP7, and LSMOP8 benchmark problems is illustrated in Figure 5. As the figure indicates, the proposed algorithm achieves superior IGD values and exhibits the fastest convergence rate, which is particularly evident when the number of function evaluations reaches 1,000. The comparative algorithms generally fail to match the performance of the proposed algorithm even after 2,000 evaluations. Beyond convergence, computational efficiency is a crucial consideration for practical applications. Figure 6 presents the average running time of all compared algorithms on ZDT6, LSMOP7, LSMOP8, and LSMOP9, with the number of decision variables ranging from 250 to 5,000.

The convergence analysis, coupled with the assessment of running time, underscores the advantages of our algorithm in addressing complex multi-objective optimization problems. Although the proposed PPM requires an additional pre-training phase, several important considerations justify this aspect. Firstly, during the fine-tuning process, the algorithm’s time consumption is comparable to that of most non-surrogate MOEAs, as opposed to ABSAEA and CSEA, which often require over a day to solve a single complex MOP. Secondly, when evaluating the algorithm’s quantitative performance in relation to the time spent on calculations, the overall computation time remains acceptable for practical problem-solving purposes. Thirdly, the time complexity of the PPM is not directly related to the dimension, thanks to the designed dimension embedding. Consequently, higher dimensions yield greater advantages. Lastly, the proposed algorithm utilizes a transformer model that can be accelerated by a GPU,

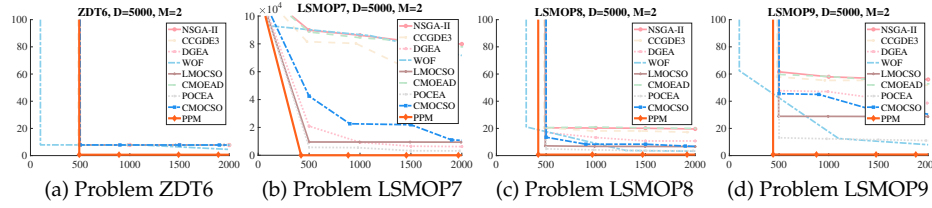


Figure 5: Visualization of Convergence of the Proposed PPM and Compared Algorithms

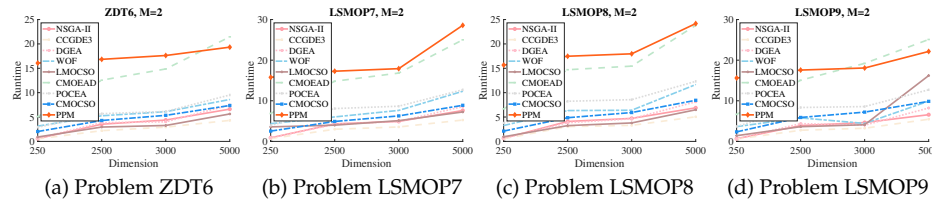


Figure 6: Visualization of the Running Time of the Proposed PPM and Compared Algorithms.

opening the possibility of investigating faster models that leverage advanced inference speeds in future research endeavors (Leviathan et al., 2023).

5 Conclusion and Future Work

Evolution and populations constitute the foundational mechanisms of heuristic MOEAs, where algorithmic efficacy critically depends on population quality. This study demonstrates the potential of population pre-training to learn evolutionary patterns from previously solved optimization problems, resulting in a unified framework capable of generating high-quality solutions for complex MOPs. Specifically, addressing limitations in existing methods concerning the modeling of large-scale populations and the integration of objective space information, we introduce dimension embedding and objective fusion techniques. The proposed Population Pre-trained Model represents an innovative approach integrating learned evolutionary pattern extraction via artificial neural networks into evolutionary computation.

Experimental results confirm the effectiveness of the proposed pre-training paradigm in solving a wide range of complex MOPs, including those characterized by large-scale decision variables, many objectives, constraints, and computationally expensive evaluation functions. The ability of PPM to generalize across diverse problem types, from constrained to large-scale MOPs, constitutes a significant advancement in evolutionary computation. Future research should explore larger-scale models and alternative neural architectures to address the challenges inherent in complex MOPs.

References

- Antonio, L. M. and Coello, C. A. C. (2013). Use of cooperative coevolution for solving large scale multiobjective optimization problems. In *2013 IEEE Congress on Evolutionary Computation*, pages 2758–2765.
- Bernardes, J., Vieira, F., Zaverucha, G., and Carbone, A. (2015). A multi-objective optimization approach accurately resolves protein domain architectures. *Bioinformatics*, 32(3):345–353.
- Brown, T., Mann, B., Ryder, N., Subbiah, M., Kaplan, J. D., Dhariwal, P., Neelakantan, A., Shyam, P., Sastry, G., Askell, A., Agarwal, S., Herbert-Voss, A., Krueger, G., Henighan, T., Child, R., Ramesh, A., Ziegler, D., Wu, J., Winter, C., Hesse, C., Chen, M., Sigler, E., Litwin, M., Gray, S., Chess, B., Clark, J., Berner, C., McCandlish, S., Radford, A., Sutskever, I., and Amodei, D. (2020). Language models are few-shot learners. In Larochelle, H., Ranzato, M., Hadsell, R., Balcan, M., and Lin, H., editors, *Advances in Neural Information Processing Systems*, volume 33, pages 1877–1901. Curran Associates, Inc.
- Cheng, R., Jin, Y., Olhofer, M., and Sendhoff, B. (2017). Test problems for large-scale multiobjective and many-objective optimization. *IEEE Transactions on Cybernetics*, 47(12):4108–4121.
- Chugh, T., Sindhya, K., Hakanen, J., and Miettinen, K. (2019). A survey on handling computationally expensive multiobjective optimization problems with evolutionary algorithms. *Soft Computing*, 23(9):3137–3166.
- Coello Coello, C. (2006). Evolutionary multi-objective optimization: a historical view of the field. *IEEE Computational Intelligence Magazine*, 1(1):28–36.
- Deb, K., Agrawal, R. B., et al. (1995). Simulated binary crossover for continuous search space. *Complex systems*, 9(2):115–148.
- Deb, K. and Jain, H. (2014). An evolutionary many-objective optimization algorithm using reference-point-based nondominated sorting approach, part i: Solving problems with box constraints. *IEEE Transactions on Evolutionary Computation*, 18(4):577–601.
- Deb, K., Pratap, A., Agarwal, S., and Meyarivan, T. (2002). A fast and elitist multiobjective genetic algorithm: Nsga-ii. *IEEE Transactions on Evolutionary Computation*, 6(2):182–197.
- Deng, Q., Kang, Q., Zhang, L., Zhou, M., and An, J. (2023). Objective space-based population generation to accelerate evolutionary algorithms for large-scale many-objective optimization. *IEEE Transactions on Evolutionary Computation*, 27(2):326–340.
- Dosovitskiy, A., Beyer, L., Kolesnikov, A., Weissenborn, D., Zhai, X., Unterthiner, T., Dehghani, M., Minderer, M., Heigold, G., Gelly, S., Uszkoreit, J., and Houlsby, N. (2021). An image is worth 16x16 words: Transformers for image recognition at scale. In *International Conference on Learning Representations*.
- Emmerich, M., Giannakoglou, K., and Naujoks, B. (2006). Single- and multiobjective evolutionary optimization assisted by gaussian random field metamodels. *IEEE Transactions on Evolutionary Computation*, 10(4):421–439.
- Graves, A. (2013). Generating sequences with recurrent neural networks. *arXiv preprint arXiv:1308.0850*.
- Gu, H., Wang, H., He, C., Yuan, B., and Jin, Y. (2024). Large-scale multiobjective evolutionary algorithm guided by low-dimensional surrogates of scalarization functions. *Evolutionary Computation*, pages 1–26.
- Gu, H., Wang, H., and Jin, Y. (2023). Effects of pareto set on the performance of problem reformulation-based large-scale multiobjective optimization algorithms. In *2023 IEEE Congress on Evolutionary Computation (CEC)*, pages 1–8.

- Habib, A., Singh, H. K., Chugh, T., Ray, T., and Miettinen, K. (2019). A multiple surrogate assisted decomposition-based evolutionary algorithm for expensive multi-/many-objective optimization. *IEEE Transactions on Evolutionary Computation*, 23(6):1000–1014.
- Han, K., Wang, Y., Chen, H., Chen, X., Guo, J., Liu, Z., Tang, Y., Xiao, A., Xu, C., Xu, Y., Yang, Z., Zhang, Y., and Tao, D. (2023). A survey on vision transformer. *IEEE Transactions on Pattern Analysis and Machine Intelligence*, 45(1):87–110.
- Haynes, W. (2013). Wilcoxon rank sum test. In Dubitzky, W., Wolkenhauer, O., Cho, K.-H., and Yokota, H., editors, *Encyclopedia of Systems Biology*, pages 2354–2355, New York, NY. Springer New York.
- He, C., Cheng, R., Tian, Y., Zhang, X., Tan, K. C., and Jin, Y. (2021). Paired offspring generation for constrained large-scale multiobjective optimization. *IEEE Transactions on Evolutionary Computation*, 25(3):448–462.
- He, C., Cheng, R., and Yazdani, D. (2022). Adaptive offspring generation for evolutionary large-scale multiobjective optimization. *IEEE Transactions on Systems, Man, and Cybernetics: Systems*, 52(2):786–798.
- He, C., Cheng, R., Zhang, C., Tian, Y., Chen, Q., and Yao, X. (2020). Evolutionary large-scale multiobjective optimization for ratio error estimation of voltage transformers. *IEEE Transactions on Evolutionary Computation*, 24(5):868–881.
- He, K., Zhang, X., Ren, S., and Sun, J. (2016). Deep residual learning for image recognition. In *Proceedings of the IEEE Conference on Computer Vision and Pattern Recognition (CVPR)*.
- Hong, H., Jiang, M., and Yen, G. G. (2024). Improving performance insensitivity of large-scale multiobjective optimization via monte carlo tree search. *IEEE Transactions on Cybernetics*, 54(3):1816–1827.
- Hong, H., Ye, K., Jiang, M., Cao, D., and Tan, K. C. (2022). Solving large-scale multiobjective optimization via the probabilistic prediction model. *Memetic Computing*, 14(2):165–177.
- Ishibuchi, H., Akedo, N., and Nojima, Y. (2015). Behavior of multiobjective evolutionary algorithms on many-objective knapsack problems. *IEEE Transactions on Evolutionary Computation*, 19(2):264–283.
- Kingma, D. P. and Ba, J. (2015). Adam: A method for stochastic optimization. In Bengio, Y. and LeCun, Y., editors, *3rd International Conference on Learning Representations, ICLR 2015, San Diego, CA, USA, May 7-9, 2015, Conference Track Proceedings*.
- Knowles, J. and Corne, D. (2007). Quantifying the effects of objective space dimension in evolutionary multiobjective optimization. In Obayashi, S., Deb, K., Poloni, C., Hiroyasu, T., and Murata, T., editors, *Evolutionary Multi-Criterion Optimization*, pages 757–771, Berlin, Heidelberg. Springer Berlin Heidelberg.
- Leviathan, Y., Kalman, M., and Matias, Y. (2023). Fast inference from transformers via speculative decoding. In Krause, A., Brunskill, E., Cho, K., Engelhardt, B., Sabato, S., and Scarlett, J., editors, *Proceedings of the 40th International Conference on Machine Learning*, volume 202 of *Proceedings of Machine Learning Research*, pages 19274–19286. PMLR.
- Li, B., Li, J., Tang, K., and Yao, X. (2015). Many-objective evolutionary algorithms: A survey. *ACM Comput. Surv.*, 48(1).
- Li, X., Wu, K., Zhang, X., Wang, H., Liu, J., et al. (2024). Pretrained optimization model for zero-shot black box optimization. *Advances in Neural Information Processing Systems*, 37:14283–14324.
- Liang, J., Ban, X., Yu, K., Qu, B., Qiao, K., Yue, C., Chen, K., and Tan, K. C. (2023). A survey on evolutionary constrained multiobjective optimization. *IEEE Transactions on Evolutionary Computation*, 27(2):201–221.

- Liu, F., Lin, X., Wang, Z., Yao, S., Tong, X., Yuan, M., and Zhang, Q. (2023). Large language model for multi-objective evolutionary optimization. *arXiv preprint arXiv:2310.12541*.
- Liu, S., Wang, Z., Lin, Q., Li, J., and Tan, K. C. (2024). Learning-aided evolutionary search and selection for scaling-up constrained multiobjective optimization. *IEEE Transactions on Evolutionary Computation*, pages 1–15.
- Luo, J., Dong, Y., Liu, Q., Zhu, Z., Cao, W., Tan, K. C., and Jin, Y. (2024). A new multitask joint learning framework for expensive multi-objective optimization problems. *IEEE Transactions on Emerging Topics in Computational Intelligence*, 8(2):1894–1909.
- Ming, F., Gong, W., Li, D., Wang, L., and Gao, L. (2023). A competitive and cooperative swarm optimizer for constrained multiobjective optimization problems. *IEEE Transactions on Evolutionary Computation*, 27(5):1313–1326.
- Neumann, A. and Neumann, F. (2024). Optimizing monotone chance-constrained submodular functions using evolutionary multiobjective algorithms. *Evolutionary Computation*, pages 1–31.
- Ouyang, L., Wu, J., Jiang, X., Almeida, D., Wainwright, C., Mishkin, P., Zhang, C., Agarwal, S., Slama, K., Ray, A., Schulman, J., Hilton, J., Kelton, F., Miller, L., Simens, M., Askell, A., Welinder, P., Christiano, P. F., Leike, J., and Lowe, R. (2022). Training language models to follow instructions with human feedback. In Koyejo, S., Mohamed, S., Agarwal, A., Belgrave, D., Cho, K., and Oh, A., editors, *Advances in Neural Information Processing Systems*, volume 35, pages 27730–27744. Curran Associates, Inc.
- Pan, L., He, C., Tian, Y., Wang, H., Zhang, X., and Jin, Y. (2019). A classification-based surrogate-assisted evolutionary algorithm for expensive many-objective optimization. *IEEE Transactions on Evolutionary Computation*, 23(1):74–88.
- Peebles, W. and Xie, S. (2023). Scalable diffusion models with transformers. In *Proceedings of the IEEE/CVF International Conference on Computer Vision*, pages 4195–4205.
- Poloni, C., Giurgevich, A., Onesti, L., and Pediroda, V. (2000). Hybridization of a multi-objective genetic algorithm, a neural network and a classical optimizer for a complex design problem in fluid dynamics. *Computer Methods in Applied Mechanics and Engineering*, 186(2):403–420.
- Qian, H. and Yu, Y. (2017). Solving high-dimensional multi-objective optimization problems with low effective dimensions. *Proceedings of the AAAI Conference on Artificial Intelligence*, 31(1).
- Seiler, M. V., Kerschke, P., and Trautmann, H. (2025). Deep-ela: Deep exploratory landscape analysis with self-supervised pretrained transformers for single-and multi-objective continuous optimization problems. *Evolutionary Computation*, pages 1–27.
- Storn, R. and Price, K. (1997). Differential evolution—a simple and efficient heuristic for global optimization over continuous spaces. *Journal of global optimization*, 11:341–359.
- Sun, Y., Zhang, C., Gao, L., and Wang, X. (2011). Multi-objective optimization algorithms for flow shop scheduling problem: a review and prospects. *The International Journal of Advanced Manufacturing Technology*, 55(5):723–739.
- Tian, Y., Cheng, R., Zhang, X., and Jin, Y. (2017). Platemo: A matlab platform for evolutionary multi-objective optimization [educational forum]. *IEEE Computational Intelligence Magazine*, 12(4):73–87.
- Tian, Y., Liu, R., Zhang, X., Ma, H., Tan, K. C., and Jin, Y. (2021a). A multipopulation evolutionary algorithm for solving large-scale multimodal multiobjective optimization problems. *IEEE Transactions on Evolutionary Computation*, 25(3):405–418.
- Tian, Y., Si, L., Zhang, X., Cheng, R., He, C., Tan, K. C., and Jin, Y. (2021b). Evolutionary large-scale multi-objective optimization: A survey. *ACM Comput. Surv.*, 54(8):1–34.
- Tian, Y. and Zhang, X. (2019). *Evolutionary Algorithm for Solving Complex Multiobjective Optimization Problems*, chapter Chapter 4, pages 107–132. World Scientific.

- Tian, Y., Zheng, X., Zhang, X., and Jin, Y. (2020). Efficient large-scale multiobjective optimization based on a competitive swarm optimizer. *IEEE Transactions on Cybernetics*, 50(8):3696–3708.
- Vaswani, A., Shazeer, N., Parmar, N., Uszkoreit, J., Jones, L., Gomez, A. N., Kaiser, L. u., and Polosukhin, I. (2017). Attention is all you need. In Guyon, I., Luxburg, U. V., Bengio, S., Wallach, H., Fergus, R., Vishwanathan, S., and Garnett, R., editors, *Advances in Neural Information Processing Systems*, volume 30. Curran Associates, Inc.
- Wang, B., Sun, Y., Xue, B., and Zhang, M. (2019). Evolving deep neural networks by multi-objective particle swarm optimization for image classification. In *Proceedings of the Genetic and Evolutionary Computation Conference, GECCO '19*, page 490–498, New York, NY, USA. Association for Computing Machinery.
- Wang, X., Jin, Y., Schmitt, S., and Olhofer, M. (2020). An adaptive bayesian approach to surrogate-assisted evolutionary multi-objective optimization. *Information Sciences*, 519:317–331.
- Wang, Z., Hong, H., Ye, K., Zhang, G.-E., Jiang, M., and Tan, K. C. (2021). Manifold interpolation for large-scale multiobjective optimization via generative adversarial networks. *IEEE Transactions on Neural Networks and Learning Systems*, pages 1–15.
- While, L., Hingston, P., Barone, L., and Huband, S. (2006). A faster algorithm for calculating hypervolume. *IEEE Transactions on Evolutionary Computation*, 10(1):29–38.
- Wu, Y., Ge, F., Chen, D., and Shi, L. (2025). Solving many-objective optimization problems based on pf shape classification and vector angle selection. *Evolutionary Computation*, pages 1–42.
- Yan, X. and Jin, Y. (2024). Emodm: A diffusion model for evolutionary multi-objective optimization. *arXiv preprint arXiv:2401.15931*.
- Zille, H., Ishibuchi, H., Mostaghim, S., and Nojima, Y. (2018). A framework for large-scale multiobjective optimization based on problem transformation. *IEEE Transactions on Evolutionary Computation*, 22(2):260–275.
- Zitzler, E., Deb, K., and Thiele, L. (2000). Comparison of multiobjective evolutionary algorithms: Empirical results. *Evolutionary Computation*, 8(2):173–195.
- Zitzler, E., Thiele, L., Laumanns, M., Fonseca, C. M., and Fonseca, V. G. d. (2003). Performance assessment of multiobjective optimizers: an analysis and review. *IEEE Transactions on Evolutionary Computation*, 7(2):117–132.

A Supplementary Material for Experiments

This is the supplementary material for the paper “Enhancing Generalization and Scalability for Multi-Objective Optimization with Population Pre-Training”, and this file includes five sections, 3 tables, and 7 figures.

This supplementary material is mainly the appendix of the experiment and is divided into two parts. Section B presents parameters in all algorithms. Section C supplements the visualization results on ZDT6 and LSMOP7-9. Sections D and E present results on benchmark LSMOP*.

B Parameter Settings

The Table 8 lists the specific parameters for each compared algorithms.

Table 8: Specific parameters for each compared algorithms

Algorithm	Reference	Parameters	Property
NSGA-II	(Deb et al., 2002)	The simulated binary crossover and the polynomial mutation are adopted; The distribution index of crossover is set to 20; The distribution index of mutation is set to 20; The crossover probability is set to 1.0.	
CCGDE3	(Antonio and Coello, 2013)	The number of subPopulations is 2; The times of each subpopulation is 1.	Large-scale
DGEA	(He et al., 2022)	The number of sampling solutions in control variable analysis is 20; The maximum number of tries required to judge the interaction is 6.	Large-scale Many-objective
WOF	(Zille et al., 2018)	The number of FEs for the optimization of each original problem t_1 is set to 1000; For the transferred problem, t_2 is set to 500; Parameter q is set to $M + 1$; The number of groups γ is set to 4; The fraction of function evaluations to use for the alternating weight-optimisation phase is 0.5.	Large-scale
LMOCSO	(Tian et al., 2020)		Large-scale Many-objective Constrained
CMOEA	(Deb and Jain, 2014)		Many-objective Constrained
CMOCSO	(Ming et al., 2023)	Extension factor τ is 0.05; Parameter to control the speed of reducing relaxation of constraints cp is 2;	Large-scale Constrained
POCEA	(He et al., 2021)	Parameter K controls the neighborhood size is 5	Large-scale Constrained
AB-SAEA	(Wang et al., 2020)	The parameter controlling the rate of change of penalty α is 2; Number of generations before updating Kriging models w_{max} is 20; Number of re-evaluated solutions at each generation μ is 5;	Many-objective Expensive
CSEA	(Pan et al., 2019)	Number of reference solutions k is 6; Number of solutions evaluated by surrogate model g_{max} is 3000;	Many-objective Expensive
EmoDM	(Yan and Jin, 2024)		Large-scale
MOEA/D-LO	(Liu et al., 2023)	LLM: GPT-3.5 Turbo	Many-objective
PPM	Ours	The ratio of sampling decision variables f is set to 0.2; The function evaluation e for decision variable sampling is set to $0.01 \times E$.	Large-scale Many-objective Constrained Expensive

C Visualization on Benchmark ZDT6, LSMOP7, LSMOP8, and LSMOP9

We visualize the nondominated solution sets obtained by all algorithms on LSMOP in Figures 7, 8, 9, and 10.

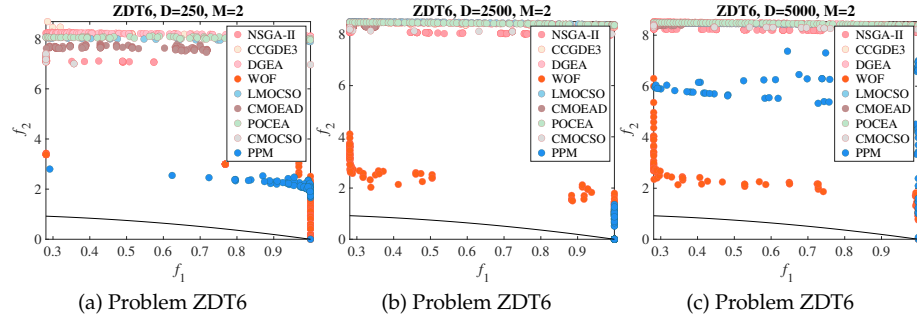


Figure 7: Visualization of Non-dominated Solutions Obtained by Each Algorithm on Bi-objective ZDT6.

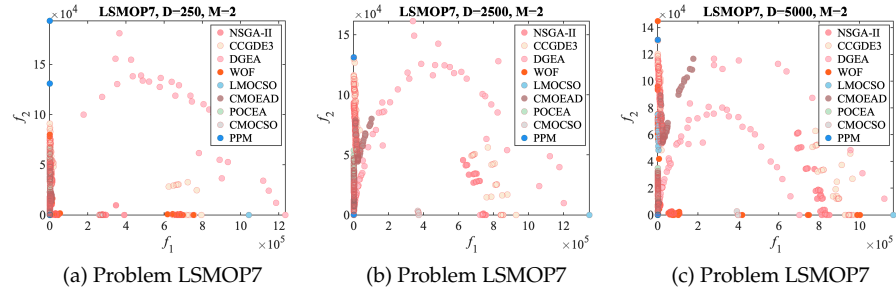


Figure 8: Visualization of Non-dominated Solutions Obtained by Each Algorithm on Bi-objective LSMOP7.

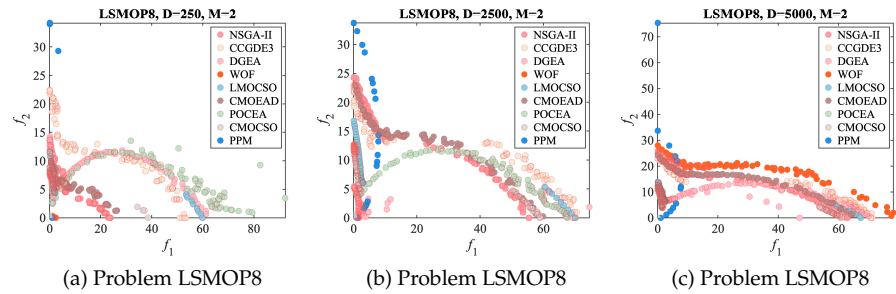


Figure 9: Visualization of Non-dominated Solutions Obtained by Each Algorithm on Bi-objective LSMOP8.

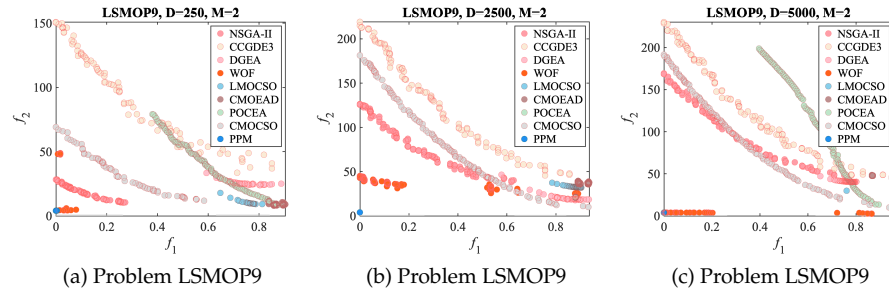


Figure 10: Visualization of Non-dominated Solutions Obtained by Each Algorithm on Bi-objective LSMOP9.

D Test on Benchmark LSMOP*

We further evaluated the performance of our proposed algorithm using the LSMOP* benchmark (Gu et al., 2023), a variant of the original LSMOP benchmark that incorporates a translation transformation.

Solutions of original LSMOP1-LSMOP9 near the boundary points **o** or **t** are proximate to or part of the PS, therefore most large-scale MOEAs can readily locate solutions near **o** or **t** by exploring specified directions and consistently achieving satisfactory results. The modified benchmark LSMOP* introduces a translation transformation to circumvent these ‘shortcuts’.

We present the experimental results on bi-objective and tri-objective LSMOP* in Tables 9 and 10, respectively. Following previous experiments, the proposed PPM is only pre-evolved on the original LSMOP1-6 and ZDT1-5. Under this modification to the benchmark, the proposed algorithm still finds better solutions on more problems (8 and 9 best results, respectively).

Table 9: IGD Values Obtained By Compared Algorithms on 27 Bi-objective Instances From LSMOP* Test Suite. The Best Result in Each Row is Highlighted in Bold.

Problem	D	NSGI-II	CCGDE3	DGEA	WOF	LMOCSSO	CMOESD	POCEA	CMOCSO	PPM
LSMOPS1	1000	6.05e+01-	6.23e+01-	5.60e+01-	5.47e+01-	5.66e+01-	6.22e+01-	5.43e+01-	5.67e+01-	4.50e+01
	2000	6.20e+01-	6.39e+01-	5.78e+01-	5.50e+01-	5.67e+01-	6.56e+01-	5.57e+01-	5.66e+01-	4.51e+01
	5000	6.49e+01-	6.46e+01-	4.08e+01+	6.46e+01-	5.72e+01=	6.68e+01-	5.61e+01+	5.74e+01-	5.72E+01
LSMOPS2	1000	6.28e-02=	6.31e-02=	6.20e-02=	5.53e-02=	6.08e-02=	6.68e-02=	5.85e-02=	6.09e-02=	6.43E-02
	2000	3.64e-02=	3.66e-02=	3.62e-02=	3.71e-02=	3.49e-02=	4.56e-02=	3.52e-02=	3.55e-02=	3.72E-02
	5000	2.01e-02=	2.03e-02=	2.00e-02=	2.02e-02=	1.95e-02=	2.98e-02=	1.98e-02=	1.98e-02=	2.24E-02
LSMOPS3	1000	1.39e+02-	1.41e+02-	1.49e+02-	1.37e+02-	7.72e+03-	1.38e+02-	1.49e+02-	1.45e+02-	5.71e+01
	2000	1.43e+02-	1.45e+02-	5.71e+01=	1.41e+02-	1.04e+05-	1.47e+02-	1.54e+02-	1.45e+02-	5.71E+01
	5000	1.48e+02-	1.50e+02-	5.71e+01=	6.48e+04-	3.57e+04-	1.53e+02-	1.60e+02-	1.47e+02-	5.71E+01
LSMOPS4	1000	1.11e-01=	1.11e-01=	1.11e-01=	1.12e-01=	1.10e-01=	1.17e-01=	1.10e-01=	1.10e-01=	1.12E-01
	2000	6.51e-02=	6.51e-02=	6.50e-02=	6.54e-02=	6.42e-02=	7.00e-02=	6.41e-02=	6.44e-02=	6.65E-02
	5000	3.32e-02=	3.33e-02=	3.29e-02=	3.37e-02=	3.28e-02=	4.55e-02=	3.30e-02=	3.29e-02=	3.45E-02
LSMOPS5	1000	1.46e+02-	1.59e+02-	1.53e+02-	1.52e+02-	1.49e+02-	1.57e+02-	1.46e+02-	1.48e+02-	9.42e+01
	2000	1.54e+02-	1.59e+02-	1.51e+02-	1.55e+02-	1.50e+02-	1.59e+02-	1.48e+02-	1.48e+02-	6.67e+01
	5000	1.58e+02-	1.62e+02-	6.67e+01+	1.47e+02+	1.51e+02+	1.66e+02-	1.46e+02+	1.48e+02+	1.52E+02
LSMOPS6	1000	8.38e-01-	8.41e-01-	8.38e-01-	8.25e-01=	3.84e+04-	1.04e+05-	8.44e-01-	8.38e-01-	7.76e-01
	2000	7.86e-01=	7.86e-01=	7.87e-01=	7.80e-01=	1.17e+04-	7.86e-01=	7.86e-01=	7.85e-01=	7.57e-01
	5000	7.58e-01=	7.58e-01=	7.48e-01=	2.10e+05-	1.91e+05-	7.58e-01=	7.58e-01=	7.58e-01=	7.48e-01
LSMOPS7	1000	9.44e+05-	1.01e+06-	1.10e+06-	4.85e+05+	6.00e+05-	9.76e+05-	5.61e+05-	6.26e+05-	5.23E+05
	2000	9.96e+05-	9.14e+05-	6.76e+05-	9.18e+05-	5.70e+05+	1.02e+06-	6.16e+05-	6.97e+05-	5.73E+05
	5000	1.08e+06-	9.53e+05-	1.06e+06-	1.02e+06-	6.22e+05+	1.11e+06-	4.97e+05+	6.44e+05+	7.12E+05
LSMOPS8	1000	6.76e+01+	7.06e+01+	6.97e+01+	6.91e+01+	6.49e+01+	7.21e+01+	5.97e+01+	6.42e+01+	7.67E+01
	2000	6.92e+01+	7.21e+01+	7.33e+01+	7.03e+01+	6.61e+01+	7.33e+01+	6.21e+01+	6.22e+01+	7.55E+01
	5000	7.38e+01+	7.34e+01+	7.65e+01-	7.42e+01+	6.28e+01+	7.60e+01-	6.07e+01+	6.57e+01+	7.57E+01
LSMOPS9	1000	1.91e+02-	2.16e+02-	1.90e+02+	1.97e+02-	1.93e+02-	1.95e+02-	1.90e+02+	1.89e+02+	1.91E+02
	2000	2.15e+02-	2.28e+02-	1.93e+02+	2.11e+02-	2.12e+02-	2.14e+02-	1.99e+02-	2.02e+02-	1.93E+02
	5000	2.27e+02-	2.41e+02-	1.93e+02+	2.03e+02-	2.24e+02-	2.32e+02-	2.00e+02-	2.09e+02-	1.93E+02
(+/-/=)		3/16/8	3/16/8	7/10/10	5/14/8	6/14/7	2/17/8	7/12/8	6/13/8	

Table 10: IGD Values Obtained By Compared Algorithms on 27 Tri-objective Instances From LSMOP* Test Suite. The Best Result in Each Row is Highlighted in Bold.

Problem	D	NSGI-II	CCGDE3	DGEA	WOF	LMOCSSO	CMOESD	POCEA	CMOCSSO	PPM
LSMOPS1	1000	6.67e+01-	7.22e+01-	6.16e+01-	6.50e+01-	6.02e+01-	6.55e+01-	5.73e+01-	6.33e+01-	4.73e+01
	2000	6.73e+01-	7.02e+01-	6.63e+01-	6.24e+01-	6.02e+01-	6.48e+01-	6.01e+01-	6.42e+01-	4.77e+01
	5000	6.94e+01-	7.12e+01-	5.14e+01-	7.02e+01-	6.23e+01-	6.89e+01-	6.07e+01-	6.45e+01-	4.73e+01
LSMOPS2	1000	8.91e-02=	8.13e-02=	8.68e-02=	8.13e-02=	7.72e-02=	8.26e-02=	8.02e-02=	7.70e-02=	8.93E-02
	2000	6.90e-02=	6.92e-02=	7.05e-02=	6.31e-02=	6.03e-02=	8.04e-02=	6.36e-02=	5.82e-02=	7.55E-02
	5000	6.07e-02=	6.10e-02=	6.04e-02=	4.97e-02=	5.02e-02=	6.29e-02=	5.63e-02=	4.85e-02=	6.78E-02
LSMOPS3	1000	1.24e+02-	9.07e+01-	3.94e+01+	1.01e+02-	8.46e+02-	8.54e+01-	1.27e+02-	1.49e+02-	5.02E+01
	2000	8.55e+01-	9.95e+01-	5.64e+01=	8.29e+01-	1.78e+03-	8.16e+01-	1.19e+02-	1.56e+02-	5.64e+01
	5000	1.16e+02-	8.46e+01-	4.78e+01+	9.27e+01-	9.83e+01-	8.40e+01-	9.87e+01-	1.53e+02-	5.63E+01
LSMOPS4	1000	1.71e-01=	1.67e-01=	1.71e-01=	1.62e-01=	1.61e-01=	1.71e-01=	1.61e-01=	1.63e-01=	1.76E-01
	2000	1.05e-01=	1.06e-01=	1.13e-01=	1.08e-01=	9.78e-02=	1.09e-01=	1.02e-01=	9.74e-02=	1.08E-01
	5000	7.69e-02=	6.99e-02=	6.68e-02=	6.04e-02=	6.23e-02=	8.42e-02=	6.34e-02=	6.02e-02=	7.58E-02
LSMOPS5	1000	1.28e+02-	1.34e+02-	1.32e+02-	1.24e+02-	1.30e+02-	1.28e+02-	1.24e+02-	1.26e+02-	5.38e+01
	2000	1.35e+02-	1.32e+02-	5.38e+01=	1.29e+02-	1.32e+02-	1.33e+02-	1.23e+02-	1.30e+02-	5.38e+01
	5000	1.36e+02-	1.34e+02-	1.33e+02-	1.38e+02-	1.27e+02-	1.36e+02-	1.27e+02-	1.31e+02-	5.37e+01
LSMOPS6	1000	3.67e+05-	4.23e+05-	3.50e+05-	3.19e+05+	3.79e+05-	3.55e+05-	2.65e+05+	3.61e+05-	3.22E+05
	2000	4.23e+05-	4.48e+05-	3.75e+05-	3.70e+05-	3.04e+05-	4.24e+05-	2.26e+05+	4.34e+05-	2.97E+05
	5000	4.50e+05+	4.93e+05+	5.75e+05+	4.72e+05+	4.31e+05+	4.26e+05+	2.58e+05+	3.86e+05+	6.04E+05
LSMOPS7	1000	1.17e+00=	1.17e+00=	1.13e+00=	1.17e+00=	1.17e+00=	1.17e+00=	1.08e+00=	1.17e+00=	1.13E+00
	2000	1.05e+00=	1.05e+00=	1.03e+00=	1.05e+00=	1.05e+00=	1.05e+00=	1.05e+00=	1.04e+00=	1.03e+00
	5000	9.83e-01=	9.83e-01=	9.76e-01=	9.82e-01=	9.82e-01=	9.83e-01=	9.82e-01=	9.83e-01=	9.76e-01
LSMOPS8	1000	9.75e-01=	9.75e-01=	9.61e-01=	9.72e-01=	9.69e-01=	7.29e-01+	9.72e-01=	9.76e-01=	9.61E-01
	2000	9.70e-01=	9.71e-01=	8.01e-01+	6.30e-01+	8.19e-01+	7.43e-01+	7.97e-01+	9.72e-01=	9.57E-01
	5000	9.67e-01=	9.66e-01=	8.91e-01+	1.19e+00-	8.02e-01+	6.94e+00-	6.94e-01+	9.70e-01=	9.54E-01
LSMOPS9	1000	4.21e+02+	4.37e+02+	4.26e+02+	4.14e+02+	4.32e+02+	4.16e+02+	4.10e+02+	4.48e+02-	4.43E+02
	2000	4.70e+02-	4.97e+02-	4.31e+02+	4.62e+02-	4.71e+02+	4.61e+02-	4.27e+02+	4.27e+02+	4.55E+02
	5000	4.85e+02-	5.08e+02-	4.25e+02+	4.19e+02+	4.68e+02-	4.82e+02-	4.29e+02+	4.36e+02+	4.40E+02
(+/-/=)		2/13/12	2/13/12	8/7/12	5/12/10	4/13/10	4/14/9	8/9/10	3/12/12	

E Visualization on Benchmark LSMOP*

We visualize the nondominated solution sets obtained by all algorithms on LSMOP* in Figures 11, 12, and 13. As can be seen from the figures, although the proposed PPM model has not been trained on LSMOP*1-9, compared with existing algorithms, it can locate solutions closer to the Pareto optimal under expensive constraints.

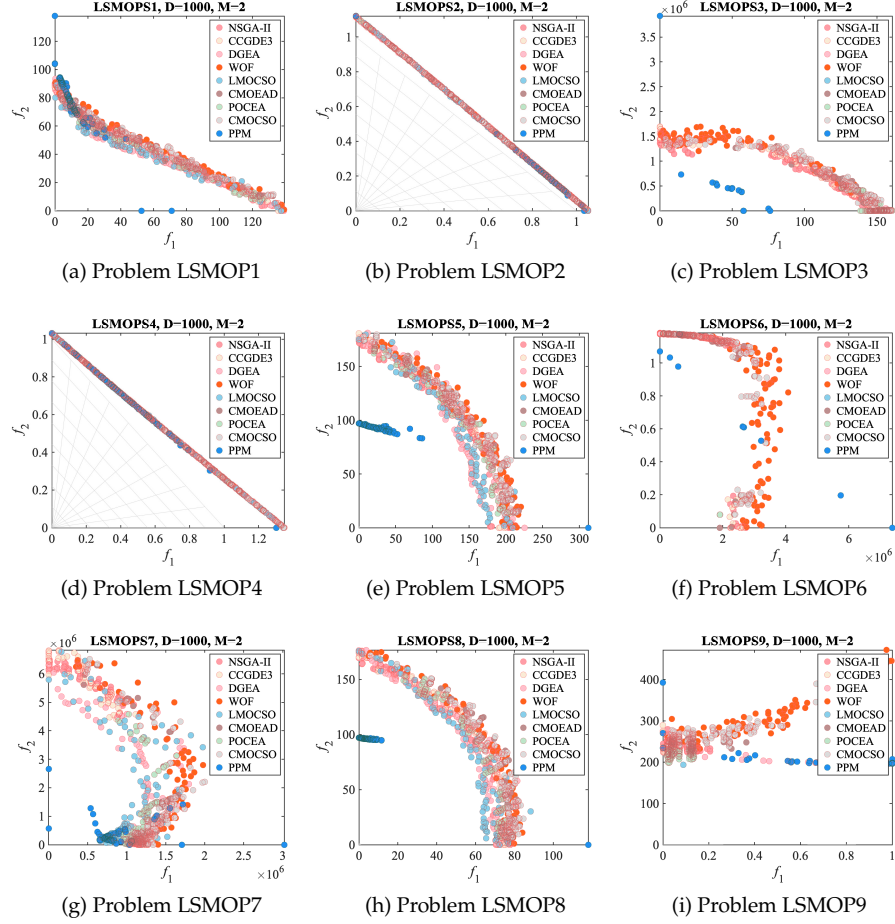


Figure 11: Visualization of Non-dominated Solutions Obtained by Each Algorithm on 1000 Dimensional Bi-objective LSMOP*1 to LSMOP*9.

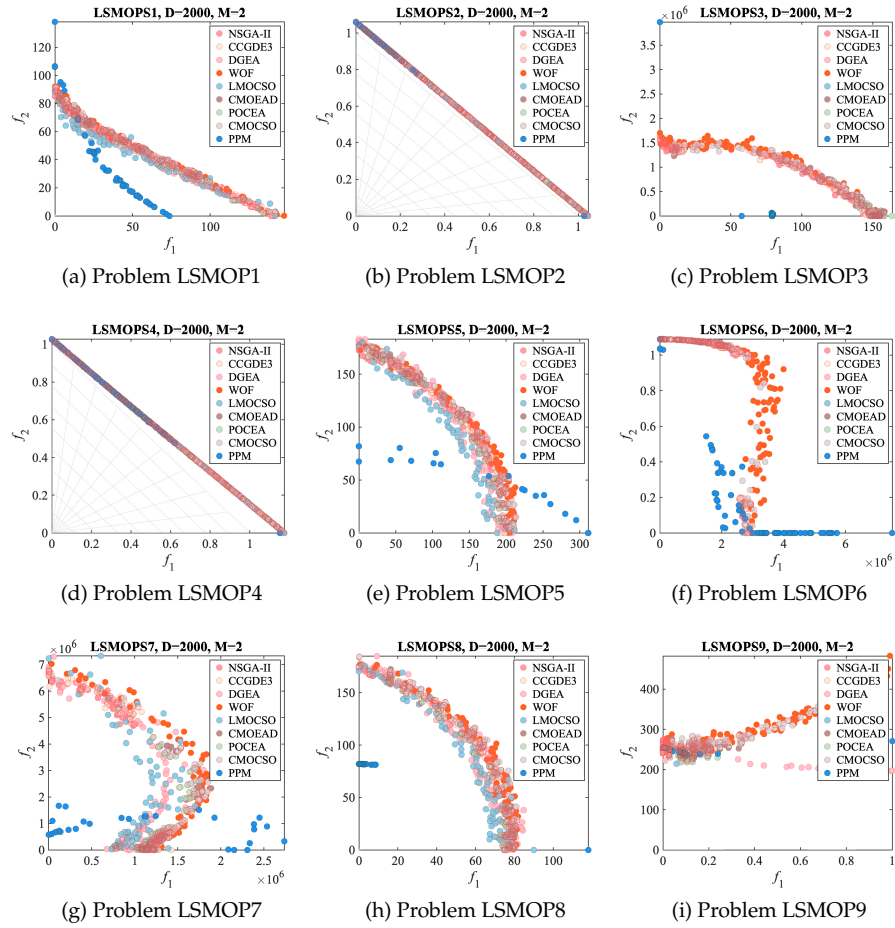


Figure 12: Visualization of Non-dominated Solutions Obtained by Each Algorithm on 2000 Dimensional Bi-objective LSMOP*1 to LSMOP*9.

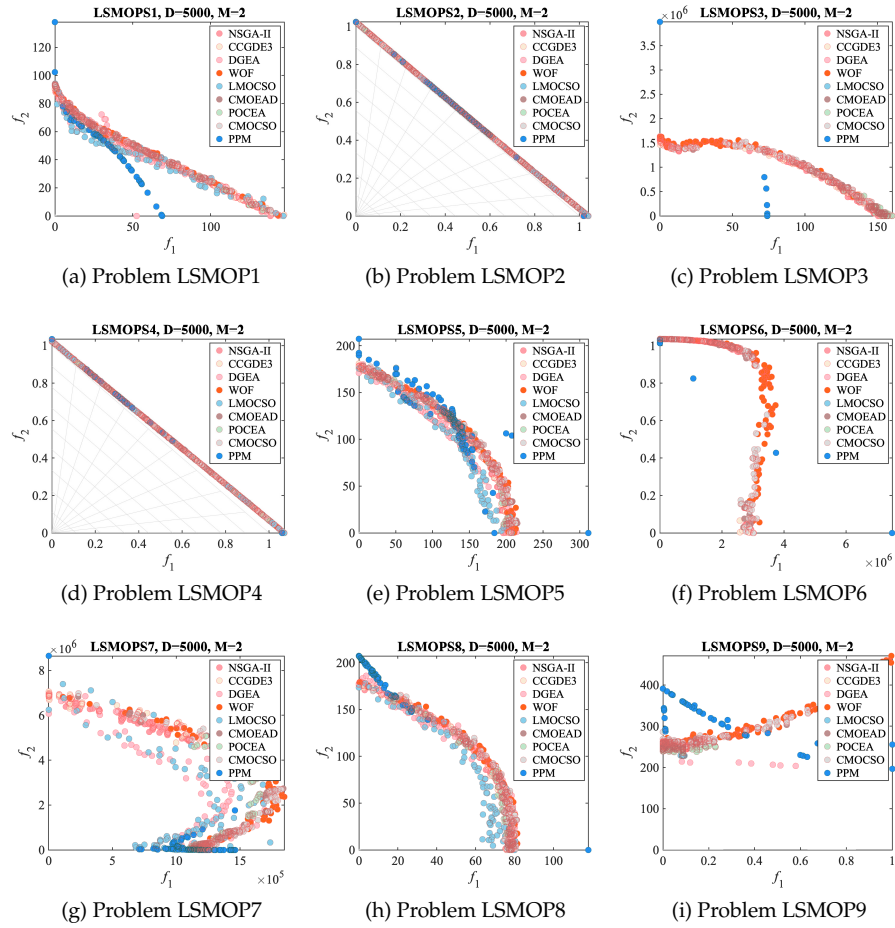


Figure 13: Visualization of Non-dominated Solutions Obtained by Each Algorithm on Bi-objective LSMOP*1 to LSMOP*9.